NeuroImage: Clinical 23 (2019) 101900

Contents lists available at ScienceDirect

NeuroImage: Clinical

journal homepage: www.elsevier.com/locate/ynicl

Specific patterns of brain alterations underlie distinct clinical profiles in Huntington's disease

Clara Garcia-Gorro[a,b,1], Alberto Llera[c,1], Saul Martinez-Horta[d,e], Jesus Perez-Perez[d,e], Jaime Kulisevsky[d,e,f], Nadia Rodriguez-Dechicha[g], Irene Vaquer[g], Susana Subira[g,h], Matilde Calopa[i], Esteban Muñoz[j,k,l], Pilar Santacruz[j], Jesus Ruiz-Idiago[m,n], Celia Mareca[m], Christian F. Beckmann[c,o], Ruth de Diego-Balaguer[a,b,p,q,*,2], Estela Camara[a,*]

[a] Cognition and Brain Plasticity Unit, L'Hospitalet de Llobregat (Barcelona), IDIBELL (Institut d'Investigació Biomèdica de Bellvitge), Spain
[b] Department of Cognition, Development and Educational Psychology, University of Barcelona, Barcelona, Spain
[c] Donders Institute for Brain, Cognition and Behaviour, Centre for Cognitive Neuroimaging, Radboud University, Nijmegen, the Netherlands
[d] Movement Disorders Unit, Department of Neurology, Hospital de la Santa Creu i Sant Pau, Biomedical Research Institute Sant Pau (IIB-Sant Pau), Barcelona, Spain
[e] CIBERNED (Center for Networked Biomedical Research on Neurodegenerative Diseases), Carlos III Institute, Madrid, Spain
[f] Universidad Autónoma de Barcelona, Barcelona, Spain
[g] Hestia Duran i Reynals, Hospital Duran i Reynals, Hospitalet de Llobregat (Barcelona), Spain
[h] Department of Clinical and Health Psychology, Universitat Autònoma de Barcelona, Barcelona, Spain
[i] Movement Disorders Unit, Neurology Service, Hospital Universitari de Bellvitge, Barcelona, Spain
[j] Movement Disorders Unit, Neurology Service, Hospital Clínic, Barcelona, Spain
[k] IDIBAPS (Institut d'Investigacions Biomèdiques August Pi i Sunyer), Barcelona, Spain
[l] Facultat de Medicina, University of Barcelona, Barcelona, Spain
[m] Hospital Mare de Deu de la Mercè, Barcelona, Spain
[n] Department of Psychiatry and Forensic Medicine, Universitat Autònoma de Barcelona, Barcelona, Spain
[o] Donders Institute for Brain, Cognition and Behaviour, Department of Cognitive Neuroscience, Radboud University Medical Center, Nijmegen, the Netherlands
[p] The Institute of Neurosciences, University of Barcelona, Barcelona, Spain
[q] ICREA (Catalan Institute for Research and Advanced Studies), Barcelona, Spain

ARTICLE INFO

Keywords:
Linked ICA
Data fusion
Huntington's disease
Neurodegeneration
Clinical profiles
Structural MRI

ABSTRACT

Huntington's disease (HD) is a genetic neurodegenerative disease which involves a triad of motor, cognitive and psychiatric disturbances. However, there is great variability in the prominence of each type of symptom across individuals. The neurobiological basis of such variability remains poorly understood but would be crucial for better tailored treatments. Multivariate multimodal neuroimaging approaches have been successful in disentangling these profiles in other disorders. Thus we applied for the first time such approach to HD. We studied the relationship between HD symptom domains and multimodal measures sensitive to grey and white matter structural alterations. Forty-three HD gene carriers (23 manifest and 20 premanifest individuals) were scanned and underwent behavioural assessments evaluating motor, cognitive and psychiatric domains. We conducted a multimodal analysis integrating different structural neuroimaging modalities measuring grey matter volume, cortical thickness and white matter diffusion indices – fractional anisotropy and radial diffusivity. All neuroimaging measures were entered into a linked independent component analysis in order to obtain multimodal components reflecting common inter-subject variation across imaging modalities. The relationship between multimodal neuroimaging independent components and behavioural measures was analysed using multiple linear regression. We found that cognitive and motor symptoms shared a common neurobiological basis, whereas the psychiatric domain presented a differentiated neural signature. Behavioural measures of different

Abbreviations: ACC, anterior cingulate cortex; CC, corpus callosum; CST, corticospinal tract; CT, cortical thickness; FA, fractional anisotropy; ICA, independent component analysis; IFOF, inferior fronto-occipital fasciculus; ILF, inferior longitudinal fasciculus; OFC, orbitofrontal cortex; PBA-s, problem behaviours assessment - short version; RD, radial diffusivity; SDMT, symbol digit modality tests; SLF, superior longitudinal fasciculus; SMA, supplementary motor area; TMT, trail making test; UF, uncinated fasciculus; UHDRS, unified Huntington's disease rating scale; VBM, voxel based morphometry

* Corresponding author at: Cognition and Brain Plasticity Unit, L'Hospitalet de Llobregat (Barcelona), IDIBELL (Institut d'Investigació Biomèdica de Bellvitge), Spain; Department of Cognition, Development and Educational Psychology, University of Barcelona, Barcelona, Spain
E-mail address: ruth.dediego@ub.edu (R. de Diego-Balaguer).
[1] The authors contributed equally to this work
[2] Lead contact: Ruth de Diego-Balaguer, 'Cognition and Brain Plasticity Unit, Feixa Llarga s/n, 08907 L'Hospitalet de Llobregat, Barcelona, Spain.

https://doi.org/10.1016/j.nicl.2019.101900
Received 29 April 2019; Received in revised form 11 June 2019
Available online 15 June 2019

symptom domains correlated with different neuroimaging components, both the brain regions involved and the neuroimaging modalities most prominently associated with each type of symptom showing differences. More severe cognitive and motor signs together were associated with a multimodal component consisting in a pattern of reduced grey matter, cortical thickness and white matter integrity in cognitive and motor related networks. In contrast, depressive symptoms were associated with a component mainly characterised by reduced cortical thickness pattern in limbic and paralimbic regions. In conclusion, using a multivariate multimodal approach we were able to disentangle the neurobiological substrates of two distinct symptom profiles in HD: one characterised by cognitive and motor features dissociated from a psychiatric profile. These results open a new view on a disease classically considered as a uniform entity and initiates a new avenue for further research considering these qualitative individual differences.

1. Introduction

Huntington's disease (HD) is a neurodegenerative disease caused by a mutation in the *HTT* gene that produces an abnormal expansion of a cytosine-adenine-guanine (CAG) trinucleotide repeat. Symptoms include motor disturbances such as chorea, dystonia and bradykinesia, cognitive deficits, especially in executive functions, and psychiatric symptoms, such as apathy and depression. Despite the monogenic nature of HD, there is a high degree of heterogeneity in the prominence and evolution of each type of symptoms experienced by HD mutation carriers.

One possible source of such interindividual differences among HD patients could be the variability in the degree of neurodegeneration of different neural circuits. In this regard, neuroimaging studies can contribute to the understanding of the neurobiological basis of phenotypic heterogeneity. However, the vast majority of neuroimaging studies in the HD literature has focused on differences from healthy controls, overlooking the interindividual differences among HD patients.. Multivariate approaches including measures of the three symptom domains simultaneously are needed to establish the specificity between brain alterations and each symptom domain (Garcia-Gorro et al., 2017). Shedding light on the specificity of this relationship is vital in order to understand disease (Aylward et al., 2013; Marquand et al., 2016). Importantly, this may also enable the development of more personalised treatments since patients with greater prominence of motor, cognitive or psychiatric impairments may have different neurobiological characteristics even though they have the same underlying genetic mutation (de Diego-Balaguer et al., 2016). With this purpose, many studies have tried to stratify patients of different disorders into subgroups. Interestingly, cellular studies on post-mortem brain tissue of HD patients have found distinctive patterns of neuronal loss associated with motor, psychiatric and mixed (motor and psychiatric) profiles (Tippett et al., 2007; Thu et al., 2010; Nana et al., 2014; Mehrabi et al., 2016). Neuroimaging techniques have been employed in neurodegenerative, psychiatric and neurodevelopmental disorders in order to subdivide patients in different profiles (Hrdlicka et al., 2005; Fair et al., 2012; Gates et al., 2014; Costa Dias et al., 2015; Drysdale et al., 2016; Lubeiro et al., 2016; Park et al., 2017). However, this has never been applied to stratify HD profiles.

Combining clinical measures of the three main types of symptoms along with different neural measures could enable us to tease apart the neural substrates of the different types of symptoms experienced by HD individuals.. Different neuroimaging modalities can provide complementary information of brain structure and microstructure to study the neuropathological substrates of HD in the same patients. Given the clinical complexity and the alterations found in both grey and white matter in HD, integrating within-subject information from different imaging modalities may provide a more complete view of the neural substrates underlying each symptom.

Multimodal neuroimaging fusion approaches enable the study of the brain from different perspectives, making use of different modalities in a single analysis, thus offering a more comprehensive view. In contrast to classical multimodal studies, where data from different modalities are analysed separately, novel multimodal fusion approaches take advantage of the common information across modalities, estimating useful features from the different modalities independently (Groves et al., 2011, 2012). This can reveal data variations not shown through the independent analyses (Abrol et al., 2017). Analysing data in a multimodal way permits the investigation of brain variability between individuals that is common across different neuroimaging modalities, thus possibly reflecting a common pathophysiologic mechanism (Francx et al., 2016). Linked independent component analysis (Linked ICA) has been successfully used to characterise brain changes in ageing (Douaud et al., 2014) and attention-deficit/hyperactivity disorder (Francx et al., 2016; Wolfers et al., 2017). It uses a data-driven multivariate approach to elucidate the hidden structure of covariance across different modalities. This type of method reduces the dimensionality of the data from thousands of voxels to a manageable number of independent components, which can be interpreted individually and characterise a biophysically plausible form of variability (Groves et al., 2012). These components can then be related to specific behavioural measures.

Thus, given the importance of distinguishing the neurobiological basis linked to different profiles in a disease such as HD with no current cure, the aim of this study was to investigate the relationship between interindividual differences in brain structure and the prominence of the three main types of symptoms in HD. We used linked ICA to merge structural neuroimaging data from different modalities including grey matter and white matter measures in order to improve the potential sensitivity in distinguishing HD profiles. We hypothesised that interindividual differences in the damage in grey and white matter regions could explain the variability in the severity of each symptom domain.

2. Material and methods

2.1. Participants

Forty-three HD mutation carriers participated in the current study between 2013 and 2017 in the area of Barcelona, Spain. HD mutation carriers were defined as carriers of the *HTT* mutation with ≥ 39 CAG repeats. Since cognitive and psychiatric symptoms as well as neural degeneration can precede the onset of motor symptoms we included manifest and premanifest individuals. Twenty-three of the gene carriers were manifest HD patients and 20 were premanifest individuals. The criterion to classify a gene carrier as manifest or premanifest was the diagnostic confidence score (DCS) of the Unified Huntington's Disease Rating Scale (UHDRS) (Huntington Study Group, 1996), with a score of four indicating manifest stage and a score of less than four considered as premanifest stage. Participants' demographic information is included in Table 1.

None of the patients had previous history of neurological disorder other than HD. All participants signed an informed consent to participate in this study, which was approved by the ethics committee of Bellvitge Institute for Biomedical Research (IDIBELL) and Bellvitge Hospital. All procedures followed were in accordance with the Helsinki Declaration of 1975.

Table 1
Mean and standard deviation of demographic and clinical information.

N total (preHD/manifest)	43 (20/23)	N
Gender (F/M)	30/13	43
Age	43.9 (11.9)	43
Education	11.7 (3.4)	42
CAG	44.2 (3.0)	42
CAP	97.6 (23.5)	42
TFC	12 (1.7)	42
Motor domain		
UHDRS-motor	13.1 (14.1)	42
Cognitive domain		
Verbal fluency	31.4 (15.1)	41
TMT B-A	93.9 (79.2)	38
SDMT	36.7 (15.7)	41
Stroop interference	3.4 (10)	39
Psychiatric domain		
Lille Apathy	−7.5 (4.6)	36
Delay discounting *k*	0.02 (0.03)	33
Depression PBA	1.8 (3)	41
Anxiety PBA	1.7 (2.5)	41
Sensitivity to reward	6.2 (3.9)	41
Sensitivity to punishment	10 (6.6)	41

Age and education are given in years. PreHD = premanifest Huntington's disease individuals; M = males; F = females; CAP = CAG-Age product; TFC = Total functional capacity; UHDRS-motor = Unified Huntington's disease rating scale total motor score; TMT B-A = Trail Making Tests B-A; SDMT = Symbol Digit Modality Test. PBA = Problem Behaviours Assessment.

2.2. Symptom assessments

Participants were evaluated in the three symptom domains (motor, cognitive and psychiatric) using a battery of clinical scales and questionnaires. The clinical assessment was carried out using the UHDRS, which comprises motor, cognitive and behavioural subscales. The UHDRS total motor score was selected as a measure of motor disability, with higher scores indicating more severe motor impairment. The cognitive domain was assessed with measures of cognitive flexibility (trail making test (TMT) B-A (Tombaugh, 2004)), verbal fluency (phonemic letter fluency test FAS (Butters et al., 1986)), inhibitory control (Stroop interference (Golden, 1978)), psychomotor speed (symbol digit modalities test, SDMT (Benedict et al., 2017)). In this case, higher scores in TMT B-A and Stroop interference indicate worse performance, while for verbal fluency and SDMT poorer performance corresponds to lower scores. Psychiatric measures included the Depression and Anxiety subscales of the short version of the Problem Behavioural Assessment (PBA-s (McNally et al., 2015)), multiplying frequency by severity, with higher scores indicating more severe symptoms, as well as the Spanish version of the sensitivity to punishment and sensitivity to reward questionnaire (SPSRQ (Torrubia et al., 2001)), with higher scores indicating more sensitivity, and the short Lille apathy scale (Sockeel et al., 2006), with higher scores indicating more severity. Due to time constrains, some of the behavioural variables were not acquired in some participants. From the behavioural database, we only included those variables in which < 15% of the data were missing. Behavioural data were windsorised in order to deal with outliers and standardised to z-scores. Missing values for each behavioural variable were replaced by the mean.

2.3. MRI data acquisition

MRI data were acquired using a 3 T whole-body MRI scanner (Siemens Magnetom Trio; Hospital Clínic, Barcelona) with a 32-channel phased array head coil. Structural images comprised a conventional high-resolution 3D T1 image (magnetisation-prepared rapid-acquisition gradient echo sequence (MPRAGE), repetition time (TR) = 1970 ms, echo time (TE) = 2.34 ms, inversion time (TI) = 1050 ms, flip angle = 9°, 1 mm isotropic voxels, 208 sagittal slices, matrix = 208 × 256 × 256, field of view (FOV) = 256 mm × 256 mm, slice thickness = 1 mm).

Diffusion weighted MRI (DW-MRI) data were acquired using a diffusion tensor imaging sequence using a dual spin-echo diffusion imaging sequence with GRAPPA (reduction factor of 4) cardiac gating, with TE = 92 ms, 2 mm isotropic voxels, no gap, 60 axial slices, FOV = 23.6 cm. In order to obtain the diffusion tensors, diffusion was measured along 64 non-collinear directions, using a single b-value of 1500 s/mm^2 and interleaved with 9 non-diffusion b = 0 images. To avoid chemical shift artefacts, frequency-selective fat saturation was used to suppress fat signal.

2.4. MRI data processing

2.4.1. Grey matter structure measures

2.4.1.1. Voxel-based morphometry. A voxel-based morphometric (VBM) analysis was carried out using the vbm8 toolbox (http://dbm.neuro.uni-jena.de/vbm/) in the SPM8 software package (Welcome Department of Imaging Neuroscience Group, London, UK) running on MATLAB (v12.b, Mathworks, Natick, MA). Specifically, unified segmentation (Ashburner and Friston, 2005) was applied to the structural T1-weighted images of each subject to estimate tissue grey matter probability maps. During this segmentation step, spatial regularisation (regularisation: 0.02, discrete cosine transform warp frequency cut-off of 22) was adapted to account for striatal neurodegeneration and ventricle dilatation. The resulting grey matter maps were then imported and fed into DARTEL (Ashburner, 2007) to achieve spatial normalisation into MNI space (Ashburner and Friston, 2009). These images were modulated by a non-linear component of the Jacobian determinant, allowing direct comparison of regional differences in the volume of grey matter corrected for individual brain sizes. Images were downsampled from 1.5 mm to 4 mm isotropic voxel size to reduce computational complexity. Finally, a 9.4 mm FWHM surface-based smoothing kernel was applied.

2.4.1.2. Cortical thickness. Vertex-wise cortical thickness (CT) maps were estimated using Freesurfer v6.0 software(http://surfer.nmr.mgh.harvard.edu/) by means of a fully automated surface reconstruction of the grey/white matter boundary and the pial surface (Dale et al., 1999; Fischl et al.,1999). Then, CT was calculated as the closest distance between the grey/white matter boundary and the pial surface at each vertex across the surface (Fischl & Dale, 2000). CT maps were projected onto the average subject surface (fsaverage) to align the cortical folding patterns. Finally, a 10 mm FWHM surface-based smoothing kernel was applied.

2.4.2. White matter microstructure measures

Brain extraction was performed using the FSL Brain Extractor Tool (Smith, 2002). Head motion and eddy-current correction were then performed using the FMRIB's Diffusion Toolbox (FDT) in FMRIB's Software Library (FSL, http://www.fmrib.ox.ac.uk/fsl/fdt) and the gradient matrix was rotated (Leemans and Jones, 2009).

The diffusion tensor was then reconstructed using Diffusion Toolkit's least-squares estimation algorithm for each voxel provided in Diffusion Toolkit (http://www.trackvis.org/dtk) and its corresponding eigenvalues and eigenvectors were extracted to calculate the fractional anisotropy (FA) and radial diffusivity (RD) maps. Using Tract-Based Spatial Statistics (TBSS, Smith et al., 2006) FA volumes were non-linearly aligned to the FMRIB-58_FA MNI template and skeletonised, building a skeletonised mean FA image, which contained the centres of all tracts common to all participants in the study. Subsequently, each participant's normalised FA map was projected onto this skeleton FA group thresholded at FA ≥ 0.2. This process was also applied for the RD map using the transformations previously calculated for the FA maps. Finally, the resolution of the skeleton was downsampled from 1 mm to

2 mm isotropic voxel size.

2.5. Linked independent component analysis

Linked independent component analysis (linked ICA) (Groves et al., 2011) is a multimodal multivariate analysis that allows the fusing of MRI data from different modalities into a single model to obtain independent components of inter-subject variability. Linked ICA takes into account the spatial correlation of each modality to determine the optimal weighting of each neuroimaging modality, which reflects the relative contribution of each modality to a given independent component. Each resulting component consists of a spatial pattern for each neuroimaging modality and a single subject-course, with the loadings of each participant indicating the contribution to each component.

In the current study we used linked ICA combining the four measures described above: VBM grey matter volume, cortical thickness, FA and RD. In order to obtain a robust model, an order smaller than 1/4 of the number of subjects is commonly advised (Groves et al., 2011, 2012). Given our sample size ($n = 43$), we initially ran the linked ICA model to estimate 10 components($n = 43$). Note that the automatic relevant determination (ARD) prior automatically identified a model order of 9 ICAs, using our initial choice of 10 as model order more and letting then the model itself decide on the number of components present in the data.

Spatial patterns of the independent components were converted to pseudo-z-statistics and thresholded at z = 2.3.

2.6. Relationship between neuroimaging components and behavioural measures

In order to study the association between each of the resulting independent components and the behavioural measures, a multiple linear regression analysis was performed for each behavioural measure, including each component as a predictor. Age was also included as a predictor with the aim of modelling its effect. Bonferroni correction was used in order to account for multiple comparisons, taking into account the number of behavioural variables ($n = 10$), resulting in a threshold of $P < 0.005$. Furthermore, we conducted a Chi-square test of independence in those components where statistically significant correlations with behavioural measures were found in order to analyse whether disease stage (manifest = 1, premanifest = 2) was associated with the contribution to this component (high = 1, low = 2). In order to establish two groups according to the subject's contribution to the component, the median subject loading in each component was calculated and all subjects with a lower loading were included in the “low” group, while subjects with higher loadings were included in the “high” group. The subject corresponding to the median loading was therefore excluded in each component.

3. Results

3.1. Linked independent component analysis

From the initial ten dimensional factorisation, the linked ICA automatically provided through the automatic relevant determination (ARD) priors a model order equal to nine, resulting in nine independent components, each of them reflecting a different combination of modalities' contributions. Fig. 1 illustrates the relative loading of each component, sorting the components by the relative amount of total variance explained, in descending order.

After visual inspection of the spatial maps of the different components, the first unimodal component was discarded. This first component, found in previous studies (Llera Arenas et al., 2018), reflected brain size and significantly correlated with age ($r = -0.57$, $P < 0.001$). Thus, we removed this component and included age as a predictor in the multiple linear regression analysis.

The remaining components were a combination of different neuroimaging variables, with diffusion measures dominating components 3, 5 and 6, whilst cortical thickness was predominant in component 7.

3.2. Relationship between neuroimaging components and behavioural measures

After correcting for multiple comparisons, two neuroimaging components were significantly correlated with behavioural measures. Component 2 was a clearly multimodal component with a roughly similar variance explained by CT (32%), FA (30%) and VBM (24%) and to a slightly lesser extent RD (13%). The subjects' loadings of this component significantly correlated with motor deficits reflected in the UHDRS total motor score ($r = -0.69$, $P < 0.001$) and also with cognitive measures related with processing speed (SDMT: $r = 0.59$, $P < 0.001$) and executive functions such as cognitive flexibility (TMT B-A: $r = -0.71$, $P < 0.001$) and phonemic fluency (verbal fluency test, FAS: $r = 0.63$, $P = 0.003$ (see Fig. 2). The only cognitive measure that did not correlate with this component was the measure of suppression of interference (Stroop interference). Regarding the contribution of HD individuals at different stages to this component, the Chi-square test of independence with Yate's continuity correction showed that, in this component, there was a significant association between disease stage and subject loadings (χ^2 (1) = 25.60, $P < 0.001$).

In this cognitive-motor component, cortical thickness and grey matter volume measures provided complementary information that overlapped in different areas. The pattern of reduced cortical thickness associated to more severe cognitive and motor disturbances extended to multiple regions, including areas related to executive functions and sensorimotor and visuospatial processing (Fig. 3). In particular, the most significant thinning was found in left superior temporal gyrus, the left supplementary motor area (SMA) and left premotor cortex.

While all the regions described so far showed cortical thinning associated with cognitive and motor impairments, it is worth noting that this component was associated at the same time with increased cortical thickness restricted to the anterior cingulate cortex (ACC) (Fig. 3).

The results of VBM were consistent with the cortical thickness maps, showing a pattern of reduced grey matter volume associated with worse cognitive and motor disturbances in regions involved in executive functions and sensorimotor processing, covering the caudate bilaterally, SMA, bilateral somatosensory cortex and superior parietal cortex extending to lateral occipital cortex. In contrast, the medial occipital

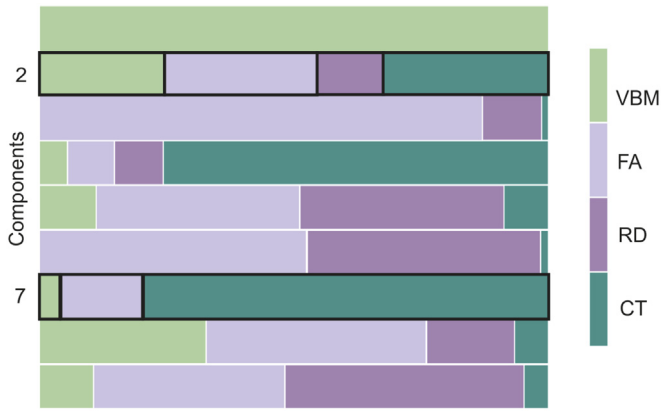

Fig. 1. Relative weight of each modality within each component. Components are sorted from 1 to 10 by the amount of variance they explain. Components that significantly correlated with behavioural measures are indicated (2 and 7). VBM = Voxel Based Morphometry; FA = Fractional Anisotropy; RD = Radial Diffusivity; CT = Cortical Thickness. Green colours relate to grey matter measures and purple colours to white matter measures. (For interpretation of the references to color in this figure legend, the reader is referred to the web version of this article.)

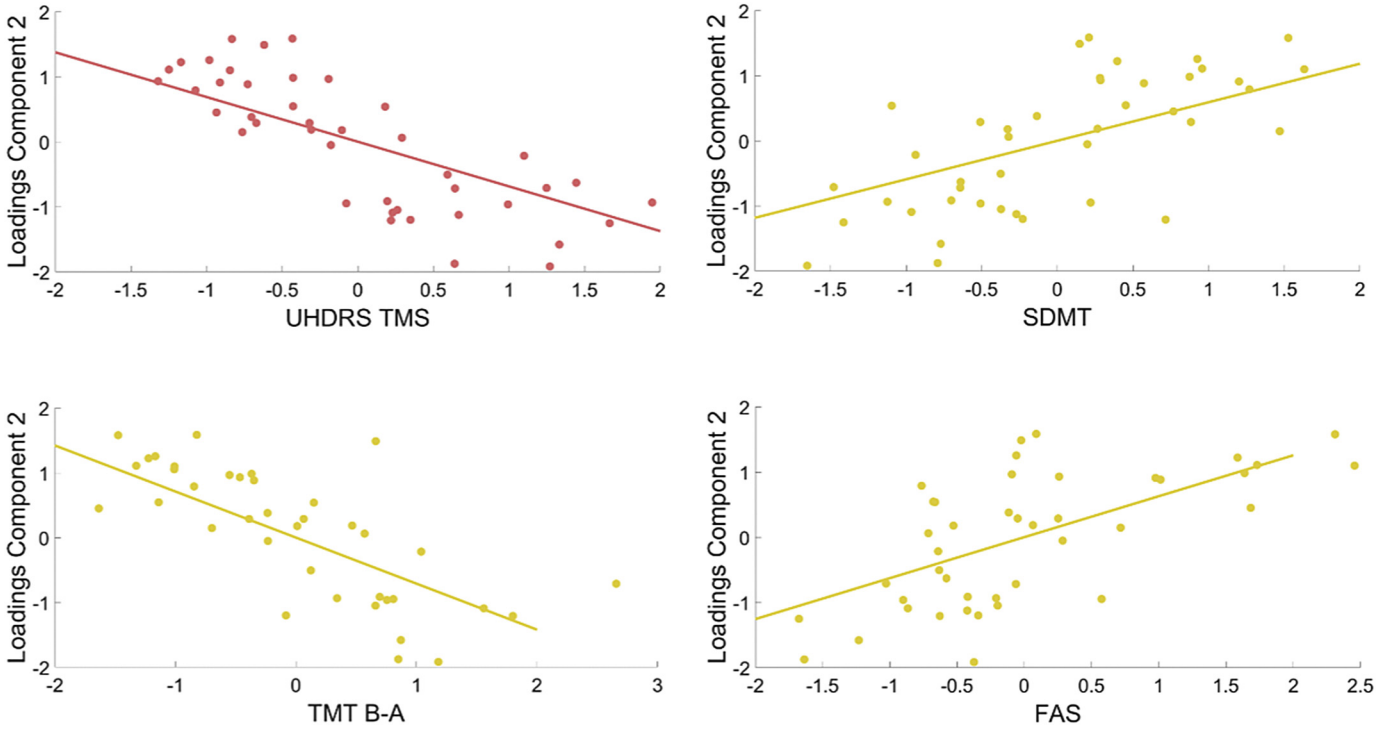

Fig. 2. Relationship between subject loadings of Component 2 and both motor (in red) and cognitive (in yellow) deficits. The plots represent betas associated with each behavioural measure in the multiple linear regression analysis. UHDRS TMS: Unified Huntington's disease Rating Scale Total Motor Scale; SDMT = Symbol Digit Modality Test; TMT B-A = Trail Making Test B-A; FAS = Phonemic fluency test (letters F, A, S). (For interpretation of the references to color in this figure legend, the reader is referred to the web version of this article.)

cortex presented increased grey matter volume in this component (Fig. 3).

Furthermore, reduced FA values were also associated to more severe cognitive and motor disturbances in a main motor-related projection, the corticospinal tract (CST) bilaterally, and in connections that are involved in cognitive processing like the bilateral fornix, superior longitudinal fasciculus (SLF), inferior fronto-occipital fasciculus (IFOF) and forceps minor and body of the corpus callosum (CC) as well as in the left arcuate fasciculus.

On the other hand, more severe cognitive and motor disturbances were at the same time associated to increased FA in the bilateral cortico-ponto-cerebellar tract (Fig. 3). Notice that the spatial maps of RD values showed, as expected, a similar inverse pattern of FA maps, where regions of reduced FA corresponded with increased RD.

The whole multimodal pattern of this cognitive-motor component is convergent, since the white matter tracts showing microstructural changes connect the grey matter areas associated to this component in the CT and VBM modalities.

In contrast to the previous component, a second component (component 7) was largely dominated by one modality: cortical thickness (CT = 78%, FA = 16%, VBM = 4%). Subjects loadings in this component were significantly correlated with depression scores (PBA-s depression subscale: $r = -0.45$, $P = 0.001$) (see Fig. 4). Furthermore, the Chi-square test of independence with Yate's continuity correction showed that this psychiatric component was equally represented by manifest and premanifest individuals not showing a significant association between disease stage and subject loading in this component ($\chi^2(1) = 0.86$, $P = 0.354$).

The pattern of cortical thickness was notably left lateralised (Fig. 5). More severe depressive symptoms were associated with reduced cortical thickness in limbic and paralimbic regions such as the left temporal pole, left ventromedial prefrontal cortex and bilateral insula. Furthermore, regions of the default mode network (DMN) such as the left superior frontal gyrus, left middle temporal gyrus, left anterior cingulate cortex (ACC) and posterior cingulate cortex (PCC) also presented reduced thickness in individuals with higher depression scores. Interestingly, some partial overlap with some regions associated with the previous component was also observed. Regions involved in sensorimotor processing such as left precentral and postcentral gyri and regions involved in cognitive processing, such as the left supramarginal gyrus also presented a pattern of reduced thickness in this component.

On the other hand, increased cortical thickness related to more severe depressive symptoms was observed in areas related to visuospatial processing, such as the left lateral occipital cortex and left fusiform gyrus extending to the left inferior temporal gyrus as well as the secondary somatosensory cortex (Fig. 5).

Although VBM contributed less to this component, it is worth noting that the reduced grey matter volume related to more severe depression resembled the pattern of reduced cortical thickness, although in this case the pattern was not left-lateralised. Similarly to the CT pattern, reduced grey matter volume was observed in areas involved in emotional processing, such as the left temporal pole and ventromedial prefrontal cortex and lateral orbitofrontal cortices bilaterally, as well as areas involved in cognition, such as the bilateral supramarginal gyrus and the right inferior frontal and middle temporal gyri as well as areas related to motor function, such as bilateral precentral and right postcentral gyri (Fig. 5).

Interestingly, this pattern of reduced grey matter volume was accompanied by increased grey matter volume in the right caudate, SMA, cerebellum and bilateral superior parietal lobules and the bilateral fusiform gyri extending to the inferior temporal gyri.

Regarding white matter measures, more depressive symptoms were associated with reduced FA in the forceps major of the CC, bilateral arcuate fasciculus IFOF, inferior longitudinal fasciculus (ILF), left uncinate fasciculus (UF) and cingulum, altogether connecting grey matter areas found to be affected in this component. On the other hand, this pattern of reduced FA was accompanied by increased FA in right UF, inferior cerebellar peduncle and in the forceps minor of the CC (Fig. 5).

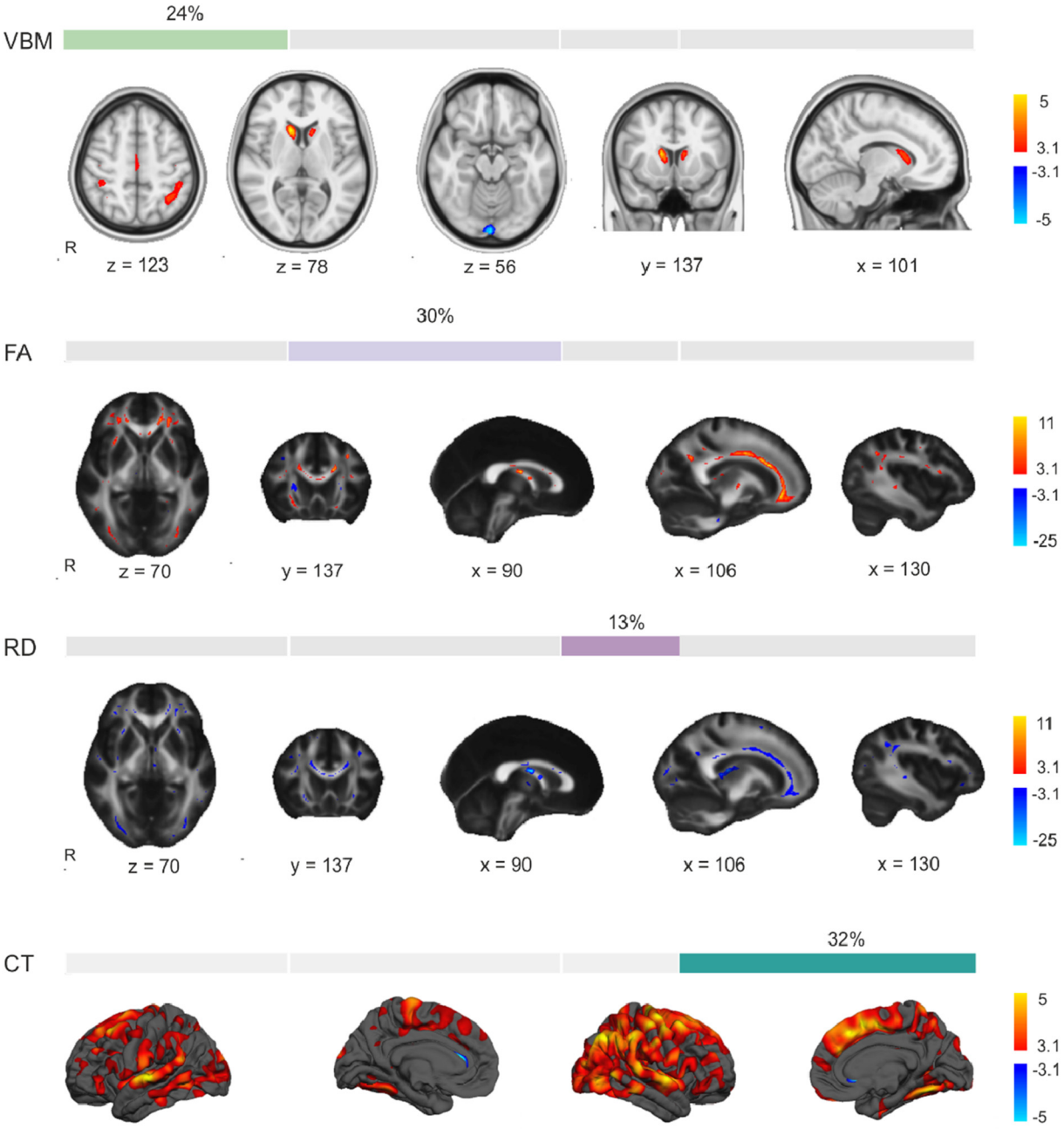

Fig. 3. Spatial maps of each modality in component 2. The percentage of variance explained by each modality in this component is indicated. Hot and cold colours indicate lower and higher values on each MRI measure associated with more cognitive and motor disturbances, respectively. Colour bars indicate *Z*-statistics. The right side of the brain is shown in the left side of the image. MNI coordinates are shown for each slice. R = Right; VBM = Voxel-based morphometry; FA = Fractional Anisotropy; RD = Radial Diffusivity; CT = Cortical Thickness. (For interpretation of the references to color in this figure legend, the reader is referred to the web version of this article.)

4. Discussion

The aim of the present study was to investigate the neurobiological basis of the three main symptom domains of HD: motor, cognitive and psychiatric disturbances. Although all of them characterise the disease, there is a high degree of heterogeneity in the prominence of each type of symptom. Thus, we hypothesised that interindividual differences in the damage in grey and white matter regions could explain the differential severity of each symptom domain. Given the complex nature of HD, with alterations in both grey and white matter, we used a multivariate and multimodal approach that allowed us to fuse images from different neuroimaging techniques and relate them with each type of symptom, in order to gain a more complete picture of the brain alterations in the disease. This approach also allowed us to see which neuroimaging modality was more sensitive in capturing the unique variance associated with each symptom domain.

We obtained four main findings. Firstly, cognitive and motor symptoms in HD shared a common neurobiological basis, whereas the psychiatric domain presents a differentiated neural signature. Secondly, cognitive and motor symptoms were associated with grey matter regions and white matter tracts involved in executive functions, language, and visuospatial and sensorimotor processing, whereas psychiatric symptoms were mainly associated with cortical areas and white matter tracts associated with emotional processing. Thirdly, whilst both grey and white matter equally contributed to explaining the cognitive-motor domain, in the case of the psychiatric domain, cortical thickness was

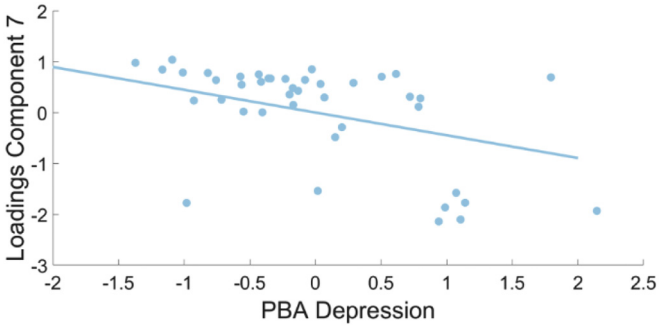

Fig. 4. Relationship between subject loadings of Component 7 and depressive symptoms. The plot represent betas associated the PBA depression behavioural measure in the multiple linear regression analysis. PBA = Problem Behaviours Assessment.

strikingly relevant compared to the other modalities. Fourthly, in the cognitive-motor component there was a higher contribution of manifest patients, while the psychiatric component was characterised by an equal contribution of both manifest and premanifest individuals.

4.1. Relationship between symptom domains and neuroimaging independent components

The first main result was that component 2 from the linked ICA correlated with scores corresponding to both motor and cognitive symptoms (processing speed, cognitive flexibility and verbal fluency), whereas component 7 correlated with a variable of the psychiatric domain: depression (Depression subscale of the PBA-s). Our findings of a common neural basis for cognitive and motor symptoms that is different from that related with the psychiatric domain is in line with a recent study (Kim et al., 2015) following symptom progression in premanifest HD individuals. In this longitudinal study, more severe motor signs were associated with worse cognitive deficits, but not always by higher levels of depressive symptoms.

4.2. Spatial maps associated with symptom domains

The second main result of this study is the difference between the spatial maps associated with the cognitive-motor domain and those of associated with the psychiatric domain. In the cognitive-motor component, more severe cognitive and motor disturbances were associated with reduced cortical thickness, volume and structural connectivity in grey matter areas and white matter tracts involved in both cognitive and motor functions. Regarding cognitive functions, the pattern of grey and white matter alterations involved structures related to cognitive control (bilateral caudate nucleus, dorsolateral prefrontal cortex, superior parietal areas), attention (SLF), visuospatial processing (occipital cortex and IFOF), language (inferior frontal areas and arcuate fasciculus) and memory (fornix). Thus, the pattern of cognitive structures involved in this component is consistent with its relationship to the

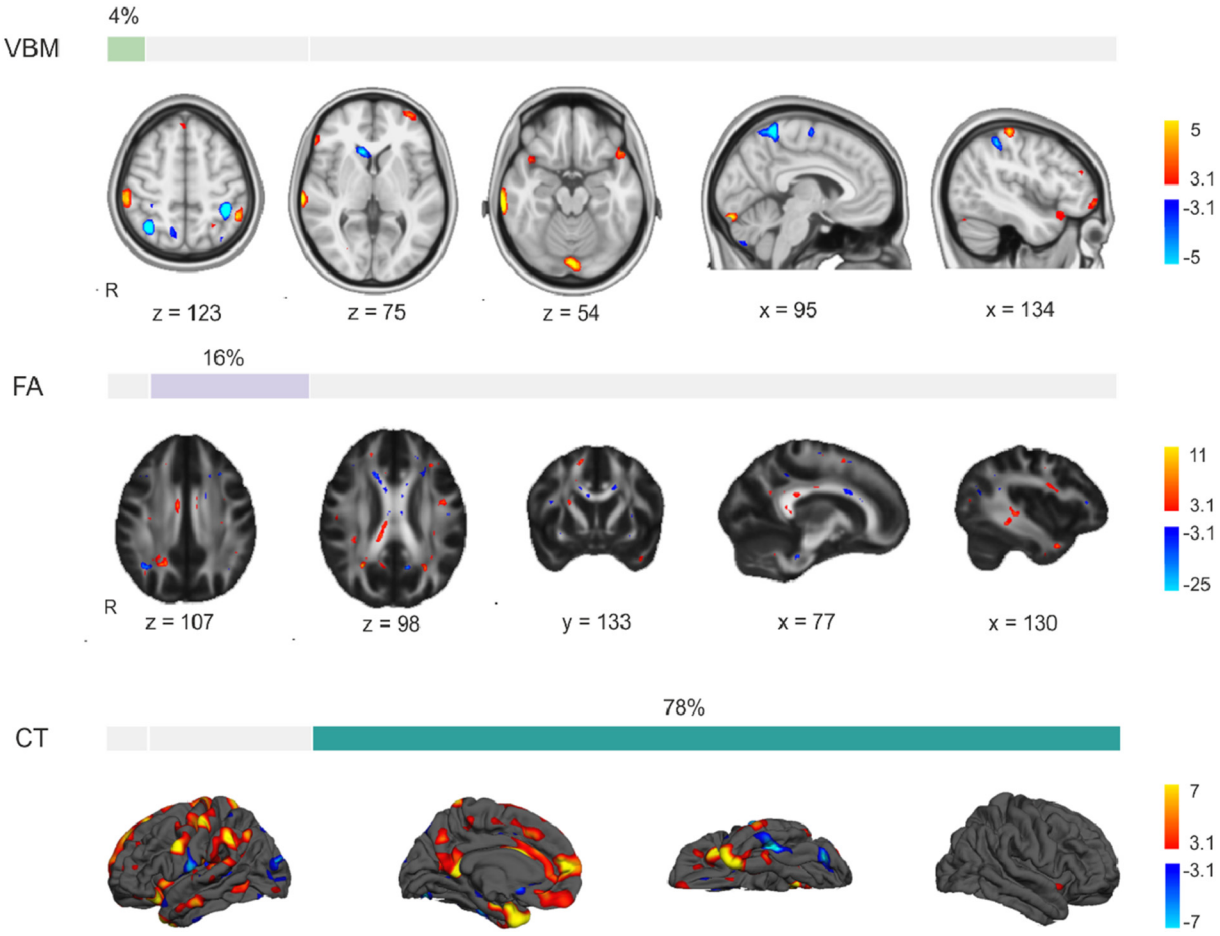

Fig. 5. Spatial maps of each modality in component 7. The percentage of variance explained by each modality in this component is indicated. Hot and cold colours indicate lower and higher values on each MRI measure associated with more depressive symptoms, respectively. Colour bars indicate *Z*-statistics. The right side of the brain is shown in the left side of the image. MNI coordinates are shown for each slice. R = Right; VBM = Voxel-based morphometry; FA = Fractional Anisotropy; RD = Radial Diffusivity; CT = Cortical Thickness. (For interpretation of the references to color in this figure legend, the reader is referred to the web version of this article.)

deficits in processing speed, cognitive flexibility and verbal fluency. Regarding the structures involved in motor function, this component showed thinning and reduced volume of the SMA and the somatosensory cortex, two key areas in motor planning and execution. The CST – a major motor tract – and the body of the CC – which connects sensorimotor regions from one hemisphere to the other – showed reduced structural connectivity in this component too. The involvement of motor areas and white matter tracts in this component is therefore in line with the observed association with motor signs.

It is important to point out that regions associated with emotional processing such as the temporal poles or the orbitofrontal cortex were not involved in this cognitive-motor component. Indeed, the only limbic structure involved, the ACC, showed a reverse pattern of cortical thickness to that of the other regions involved. Thus, the increased cortical thickness in this structure could suggest that patients with a cognitive-motor profile may be less prone to emotional disturbances.

In contrast, the spatial map of the psychiatric component was primarily characterised by a pattern of reduced grey matter thickness and volume and white matter connectivity in structures related to emotional processing. Depressive symptoms were associated with alterations in limbic and paralimbic structures previously associated with depression, such as the ACC, medial OFC, medial temporal gyrus, temporal pole and anterior insula (Lee et al., 2011; Sprengelmeyer et al., 2011; Grieve et al., 2013; Ramasubbu et al., 2014; Webb et al., 2014) as well as the cingulum bundle and the left UF (Taylor et al., 2007; Dalby et al., 2010; Schermuly et al., 2010; Keedwell et al., 2012; Zhang et al., 2012).

In the cortical thickness modality, which explained a great majority of the variance of the psychiatric component, the pattern was clearly left-lateralised, with the exception of the insula, which was found in both hemispheres. This is in line with an extensive literature on depression that shows an imbalance in interhemispheric grey matter (Koolschijn et al., 2009; Tu et al., 2012) and dynamics with hypoactivity of the left hemisphere and hyperactivity of the right hemisphere (for a review see Hecht, 2010).

In addition, the pattern of cortical thickness included the ACC, PCC, superior frontal gyrus and middle temporal gyrus, all areas pertaining to the DMN. Our results, therefore, are consistent with the known association between hyperactivity of the DMN and depression, possibly due to a maladaptive self-oriented rumination (Berman et al., 2011; Hamilton et al., 2011, 2015).

Besides structures classically associated with the processing and regulation of emotion, we also found alterations in some grey matter regions and white matter tracts associated with cognitive processing such as the left supramarginal gyrus and bilateral IFOF, arcuate fasciculus and ILF. Cortical thinning was also found in sensorimotor processing areas such as the precentral and postcentral gyri. Interestingly, cognitive and sensorimotor areas have also been found to be affected in depression, in terms of both grey matter structure (Tu et al., 2012; Grieve et al., 2013) and functional connectivity (Drysdale et al., 2016).

On the other hand, the psychiatric component was also associated with a pattern of increased grey matter. This was observed in areas related with visual processing, such as the lateral occipital and lingual cortices and cognitive control, such as the right caudate, precuneus, superior parietal cortex, cerebellum and SMA. These results suggest that these areas tend to be preserved in HD patients with depressive symptoms.

In summary, the second main finding showed large differences between the spatial maps of the cognitive-motor and the psychiatric components, with a low degree of overlapping. All in all, the regions that we found to be associated with each symptom component are in line with its known functions. Importantly, some regions showed opposite patterns. For instance, whilst in the cognitive-motor component more severe deficits were associated with reduced volume in right caudate, SMA and bilateral superior parietal gyrus as well as reduced cortical thickness in lateral occipital and lingual cortices, these areas showed increased volume and thickness associated with higher depression scores in the psychiatric component. On the other hand, in the cognitive-motor component, the middle occipital cortex and the ACC showed increased volume and thickness, respectively, while the inverse pattern was observed in the psychiatric component.

The results of the spatial maps partially converge with the model of segregated motor, associative and limbic cortico-striatal circuits (Parent and Hazrati, 1995; Humphries and Prescott, 2010), characterised by a partial overlap between motor and associative networks and a more clearly segregated limbic loops.

4.3. Contribution of neuroimaging modalities in each symptom profile

Regarding the third main finding of the current study, there were differences regarding the contribution of each modality to each component. In the case of the cognitive-motor component, both grey and white matter measures had a similar weight, whereas the psychiatric component was clearly dominated by a single modality: cortical thickness.

These results may suggest differences in the pathophysiology underlying different symptoms in HD. On the one hand, cognitive and motor symptoms seem to be caused equally by a reduction in grey matter volume, cortical thickness and white matter integrity. In contrast, the neural underpinning of depression in HD seems to be much more restricted, primarily involving cortical thickness with grey matter volume only explaining 4% of the variance.

It is important to note that, even though cortical thickness influences grey matter volume, these two measures are independent, since grey matter volume also depends of surface area, which is thought to contribute to a larger extent than cortical thickness (Winkler et al., 2010). Although the neurobiological basis of each metric is still unclear, it has been observed that in many, but not all, cortical regions of the brain thicker areas have reduced neural density (la Fougère et al., 2011), which is thought to indicate an increased number of dendrites and synapses per neuron (Wagstyl et al., 2015). Thus, in many brain regions, cortical thickness could be related to cortical connectivity (Chiarello et al., 2016).

4.4. Contribution of premanifest and manifest individuals in each symptom domain

The fourth main finding of the study showed that subject loadings which contributed more to the cognitive-motor component included significantly more manifest patients than premanifest individuals, while in the psychiatric component the subjects who contributed more to the component were a mix of manifest and premanifest individuals. This is in line with the previous studies that have found that whilst cognitive and motor deficits tend to worsen as the disease progresses (Mahant et al., 2003; Stout et al., 2011), depressive symptoms can vary across different disease stages and do not correlate with disease progression (Craufurd et al., 2001; Julien et al., 2007; Kim et al., 2015).

4.5. Integration of main findings and concluding remarks

Considering the four main findings of our study which show differences between cognitive-motor and psychiatric domains regarding i) the associations with independent components, ii) brain structures involved, iii) contributions of each neuroimaging modality and iv) contribution of patients in premanifest and manifest stages, we propose that there are two distinct symptom profiles in HD with differentiated neural substrates.

Our results suggest that depression in HD is independent of striatal degeneration, which would explain the lack of correlation between depression and disease progression. This division of psychiatric symptoms from cognitive and motor disturbances could originate from the differences in the cortico-striatal circuits involved. In both cognitive

and motor circuits, cortical areas (dorsolateral prefrontal and sensorimotor cortices, respectively) project to the dorsal striatum (caudate and putamen), while in the limbic circuit, cortical areas (mainly the ACC) project to the ventral striatum. In addition, the output of basal ganglia nuclei are also distinct. Whilst in cognitive and motor circuits projections from the dorsal striatum connect to the dorsal portions of the globus pallidus, the limbic circuit projects to the ventral pallidum. Furthermore, the dopaminergic pathways involved are also different. In the cognitive and motor circuits, dopaminergic projections from the substantia nigra pars compacta connect to the dorsal striatum through the nigrostriatal pathway. In the case of the limbic circuit, the ventral striatum receives dopaminergic projections from the ventral tegmental area through the mesolimbic pathway.

The interaction between the cognitive and the motor circuits has been repeatedly observed in the literature. Some instances are the role of executive prefrontal regions in gait speed control (Suzuki et al., 2004) and the involvement of pre-SMA in cognitive motor control (Ikeda et al., 1999), being an area at the intersection of cognitive and motor domains. Furthermore, it has been observed that there is greater influence of cognitively demanding contexts in motor performance during cognitive-motor dual tasks in older adults (Oliveira et al., 2018) and different neurological populations, such as stroke (Plummer et al., 2013) and Parkinson's disease patients (Kelly et al., 2012), which further highlights the possibility that shared neural circuits could underlie the relationship between cognitive and motor functions. Another example of this interaction is the engagement of both executive and motor corticostriatal circuits during learning (Wang et al., 2017).

Thus, given the high degree of interaction and overlap between the cognitive and motor systems, it is plausible that alterations in both circuits form the neural basis of a shared symptom profile comprising cognitive and motor deficits in HD that is distinct from the psychiatric profile.

Regarding depression in HD, there is still debate in relation to its source. In a study on at-risk individuals undergoing genetic testing, HD gene-carriers presented higher depression rates than those who turned out negative for HD (Julien et al., 2007). This result suggests that there is a relationship between depression and the neuropathology of HD. However, in a more recent study, depression prevalence in manifest and premanifest individuals was comparable to their care-givers or people with a history of being at-risk for HD but genetically confirmed to be non-carriers (Martinez-Horta et al., 2016). In addition, the fact that depression scores in general do not correlate with clinical or biological indicators of disease progression has been suggested to be an indication that this psychiatric symptom is not linked to the neuropathology of HD (Sprengelmeyer et al., 2014).

Previous neuroimaging studies investigating the relationship between the three different symptom domains and brain structure at whole-brain level in HD have not found an association with psychiatric symptoms (Aylward et al., 2013; Scahill et al., 2013). Our results suggest that this relationship is preferentially captured by cortical thickness measures and that classical univariate analysis may have insufficient power to detect it when including multiple symptom measures and whole brain level analysis. We found that the neural basis of depression in HD share commonalities with those found in major depression disorder.

Finally, the current study presents the limitation of only including structural measures of the brain. Given the sample size, it was not advisable to include more neuroimaging modalities in the linked ICA in order to maintain a sufficient number of degrees of freedom. Future studies with larger sample sizes could nonetheless incorporate resting-state functional connectivity measures with the aim of better understanding the contribution of each type of neurobiological changes to the complex symptomatology of HD.

In conclusion, using a multivariate multimodal approach we were able to distinguish two symptom profiles in HD (cognitive-motor and psychiatric) with different neurobiological basis. These results are relevant in the context of clinical trials, since they could be used to define specific biomarkers for each symptom profile, even before clinical signs appear. Having more homogenous groups would potentially increase the likelihood of detecting successful interventions and help to find individualised treatments that target specific cognitive, motor and psychiatric disturbances. Furthermore, our findings underscore the value of multimodal fusion approaches in characterising heterogeneous patterns of neurodegeneration.

Funding

This work was supported by the Instituto de Salud Carlos III, which is an agency of the MINECO, co-funded by European Regional Development Fund (ERDF), a way to Build Europe (CP13/00225 and PI14/00834, both to EC). This study was also funded by Ministerio de Ciencia, Innovación y Universidades, which is part of Agencia Estatal de Investigación (AEI), through the project BFU2017-87109-P to RdD (Co-funded by ERDF, a way to build Europe). We thank CERCA Programme / Generalitat de Catalunya for institutional support.

Declaration of Competing interests

The authors declare no competing interests.

Acknowledgements

We are grateful to the patients and their families for taking the time to participate in our study.

References

Abrol, A., Rashid, B., Rachakonda, S., Damaraju, E., Calhoun, V.D., 2017. Schizophrenia shows disrupted links between brain volume and dynamic functional connectivity. [Internet]. Front. Neurosci. 624 (11) [cited 2017 Dec 4] Available from. http://www.ncbi.nlm.nih.gov/pubmed/29163021.

Ashburner, J., 2007. A fast diffeomorphic image registration algorithm [Internet]. Neuroimage 38, 95–113. [cited 2018 Sep 27] Available from. http://www.ncbi.nlm.nih.gov/pubmed/17761438.

Ashburner, J., Friston, K.J., 2009. Computing average shaped tissue probability templates [Internet]. Neuroimage 45, 333–341. [cited 2018 Sep 27] Available from. http://www.ncbi.nlm.nih.gov/pubmed/19146961.

Aylward, E.H., Harrington, D.L., Mills, J.A., Nopoulos, P.C., Ross, C.A., Long, J.D., et al., 2013. Regional atrophy associated with cognitive and motor function in prodromal Huntington disease. [Internet]. J. Huntingtons. Dis. 2, 477–489. Available from. http://www.pubmedcentral.nih.gov/articlerender.fcgi?artid=4412155&tool=pmcentrez&rendertype=abstract.

Benedict, R.H., DeLuca, J., Phillips, G., LaRocca, N., Hudson, L.D., Rudick, R., et al., 2017. Validity of the Symbol Digit Modalities Test as a cognition performance outcome measure for multiple sclerosis. [Internet]. Mult. Scler. 23, 721–733. [cited 2018 Jul 23] Available from. http://www.ncbi.nlm.nih.gov/pubmed/28206827.

Berman, M.G., Peltier, S., Nee, D.E., Kross, E., Deldin, P.J., Jonides, J., 2011. Depression, rumination and the default network [Internet]. Soc. Cogn. Affect. Neurosci. 6, 548–555. [cited 2018 Feb 25] Available from. http://www.ncbi.nlm.nih.gov/pubmed/20855296.

Butters, N., Wolfe, J., Granholm, E., Martone, M., 1986. An assessment of verbal recall, recognition and fluency abilities in patients with Huntington's disease. Cortex 22, 11–32.

Chiarello, C., Vazquez, D., Felton, A., McDowell, A., 2016. Structural asymmetry of the human cerebral cortex: regional and between-subject variability of surface area, cortical thickness, and local gyrification. [Internet]. Neuropsychologia 93, 365–379. [cited 2018 Feb 26] Available from. http://www.ncbi.nlm.nih.gov/pubmed/26792368.

Costa Dias, T.G., Iyer, S.P., Carpenter, S.D., Cary, R.P., Wilson, V.B., Mitchell, S.H., et al., 2015. Characterizing heterogeneity in children with and without ADHD based on reward system connectivity [Internet]. Dev. Cogn. Neurosci. 11, 155–174. [cited 2017 Mar 21] Available from. http://linkinghub.elsevier.com/retrieve/pii/S1878929315000158.

Craufurd, D., Thompson, J.C., Snowden, J.S., 2001. Behavioral changes in Huntington disease [Internet]. Neuropsychiat. Neuropsychol. Behav. Neurol. 14, 219–226. [cited 2017 May 9] Available from. http://www.ncbi.nlm.nih.gov/pubmed/11725215.

Dalby, R.B., Frandsen, J., Chakravarty, M.M., Ahdidan, J., Sørensen, L., Rosenberg, R., et al., 2010. Depression severity is correlated to the integrity of white matter fiber tracts in late-onset major depression [Internet]. Psychiatry Res. Neuroimaging 184, 38–48. [cited 2018 Feb 25] Available from. http://www.ncbi.nlm.nih.gov/pubmed/20832255.

Dale, A.M., Fischl, B., Sereno, M.I., 1999. Cortical surface-based analysis I: segmentation

and surface reconstruction. Neuroimage 9, 179–194.
Thu, D.C.V., Oorschot, D.E., Tippett, L.J., Nana, A.L., Hogg, V.M., Synek, B.J., et al., 2010. Cell loss in the motor and cingulate cortex correlates with symptomatology in Huntington's disease [Internet]. Brain 133, 1094–1110. .[cited 2017 Mar 31] Available from. http://www.ncbi.nlm.nih.gov/pubmed/20375136.
de Diego-Balaguer, R., Schramm, C., Rebeix, I., Dupoux, E., Durr, A., Brice, A., et al., 2016. COMT Val158Met polymorphism modulates Huntington's disease progression [Internet]. PLoS One 11, e0161106 [cited 2017 Aug 14] Available from. http://www.ncbi.nlm.nih.gov/pubmed/27657697.
Douaud, G., Groves, A.R., Tamnes, C.K., Westlye, L.T., Duff, E.P., Engvig, A., et al., 2014. A common brain network links development, aging, and vulnerability to disease. [Internet]. Proc. Natl. Acad. Sci. U. S. A. 111, 17648–17653. [cited 2017 Dec 4] Available from. http://www.ncbi.nlm.nih.gov/pubmed/25422429.
Drysdale, A.T., Grosenick, L., Downar, J., Dunlop, K., Mansouri, F., Meng, Y., et al., 2016. Resting-state connectivity biomarkers define neurophysiological subtypes of depression [Internet]. Nat. Publ. Gr. 23https://doi.org/10.1038/nm.4246. Available from.
Fair, D.A., Bathula, D., Nikolas, M.A., Nigg, J.T., 2012. Distinct neuropsychological subgroups in typically developing youth inform heterogeneity in children with ADHD. [Internet]. Proc. Natl. Acad. Sci. U. S. A. 109, 6769–6774. [cited 2017 Mar 21] Available from. http://www.ncbi.nlm.nih.gov/pubmed/22474392.
Fischl, B., Sereno, M.I., Dale, A.M., 1999. Cortical surface-based analysis II: inflation, flattening, and a surface-based coordinate system. Neuroimage 9, 195–207.
Fischl, B., Dale, A.M., 2000. Measuring the thickness of the human cerebral cortex from magnetic resonance images. Proc. Natl. Acad. Sci. 97, 11044–11049.
Francx, W., Llera, A., Mennes, M., Zwiers, M.P., Faraone, S.V., Oosterlaan, J., et al., 2016. Integrated analysis of gray and white matter alterations in attention-deficit/hyperactivity disorder. [Internet]. NeuroImage. Clin. 11, 357–367. [cited 2017 Dec 4] Available from. http://www.ncbi.nlm.nih.gov/pubmed/27298764.
Garcia-Gorro, C., Camara, E., de Diego-Balaguer, R., 2017. Neuroimaging as a tool to study the sources of phenotypic heterogeneity in Huntington's disease. [Internet]. Curr. Opin. Neurol. 30, 398–404. [cited 2017 Aug 14] Available from. http://insights.ovid.com/crossref?an=00019052-201708000-00005.
Gates, K.M., Molenaar, P.C.M., Iyer, S.P., Nigg, J.T., Fair, D.A., 2014. Organizing heterogeneous samples using community detection of GIMME-derived resting state functional networks [Internet]. PLoS One 9, e91322 [cited 2017 Mar 21] Available from. http://dx.plos.org/10.1371/journal.pone.0091322.
Golden, C.J., 1978. Stroop Color and Word Test: A Manual for Clinical and Experimental Uses.
Grieve, S.M., Korgaonkar, M.S., Koslow, S.H., Gordon, E., Williams, L.M., 2013. Widespread reductions in gray matter volume in depression. [Iternet]. NeuroImage. Clin. 3, 332–339. [cited 2018 Feb 20] Available from. http://linkinghub.elsevier.com/retrieve/pii/S2213158213001162.
Groves, A.R., Beckmann, C.F., Smith, S.M., Woolrich, M.W., 2011. Linked independent component analysis for multimodal data fusion [Internet]. Neuroimage 54, 2198–2217. [cited 2017 Sep 21] Available from. http://www.ncbi.nlm.nih.gov/pubmed/20932919.
Groves, A.R., Smith, S.M., Fjell, A.M., Tamnes, C.K., Walhovd, K.B., Douaud, G., et al., 2012. Benefits of multi-modal fusion analysis on a large-scale dataset: life-span patterns of inter-subject variability in cortical morphometry and white matter microstructure [Internet]. Neuroimage 63, 365–380. [cited 2017 Jun 13] Available from. http://www.sciencedirect.com/science/article/pii/S1053811912006532.
Hamilton, J.P., Furman, D.J., Chang, C., Thomason, M.E., Dennis, E., Gotlib, I.H., 2011. Default-mode and task-positive network activity in major depressive disorder: implications for adaptive and maladaptive rumination [internet]. Biol. Psychiatry 70, 327–333. [cited 2018 Feb 25] Available from. http://www.ncbi.nlm.nih.gov/pubmed/21459364.
Hamilton, J.P., Farmer, M., Fogelman, P., Gotlib, I.H., 2015. Depressive rumination, the default-mode network, and the dark matter of clinical neuroscience [Internet]. Biol. Psychiatry 78, 224–230. [cited 2018 Feb 25] Available from. http://www.ncbi.nlm.nih.gov/pubmed/25861700.
Hecht, D., 2010. Depression and the hyperactive right-hemisphere [Internet]. Neurosci. Res. 68, 77–87. [cited 2018 Feb 19] Available from. http://www.ncbi.nlm.nih.gov/pubmed/20603163.
Hrdlicka, M., Dudova, I., Beranova, I., Lisy, J., Belsan, T., Neuwirth, J., et al., 2005. Subtypes of autism by cluster analysis based on structural MRI data [Internet]. Eur. Child Adolesc. Psychiatry 14, 138–144. [cited 2017 Mar 31] Available from. http://www.ncbi.nlm.nih.gov/pubmed/15959659.
Humphries, M.D., Prescott, T.J., 2010. The ventral basal ganglia, a selection mechanism at the crossroads of space, strategy, and reward. [Internet]. Prog. Neurobiol. 90, 385–417. [cited 2019 Feb 1] Available from. http://www.ncbi.nlm.nih.gov/pubmed/19941931.
Huntington Study Group Investigators HSG, 1996. Unified Huntington's disease rating scale: reliability and consistency [Internet]. Mov. Disord. 11, 136–142. [cited 2017 Mar 3] Available from. http://www.ncbi.nlm.nih.gov/pubmed/8684382.
Ikeda, A., Yazawa, S., Kunieda, T., Ohara, S., Terada, K., Mikuni, N., et al., 1999. Cognitive motor control in human pre-supplementary motor area studied by subdural recording of discrimination/selection-related potentials [Internet]. Brain 122, 915–931. [cited 2018 Jul 8] Available from. https://academic.oup.com/brain/article-lookup/doi/10.1093/brain/122.5.915.
Julien, C.L., Thompson, J.C., Wild, S., Yardumian, P., Snowden, J.S., Turner, G., et al., 2007. Psychiatric disorders in preclinical Huntington's disease. [Internet]. J. Neurol. Neurosurg. Psychiatry 78, 939–943. [cited 2017 Mar 17] Available from. http://www.ncbi.nlm.nih.gov/pubmed/17178819.
Keedwell, P.A., Chapman, R., Christiansen, K., Richardson, H., Evans, J., Jones, D.K., 2012. Cingulum white matter in young women at risk of depression: the effect of family history and anhedonia [Internet]. Biol. Psychiatry 72, 296–302. [cited 2018 Feb 25] Available from. http://www.ncbi.nlm.nih.gov/pubmed/22386005.
Kelly, V.E., Eusterbrock, A.J., Shumway-Cook, A., 2012. A review of dual-task walking deficits in people with Parkinson's disease: motor and cognitive contributions, mechanisms, and clinical implications [Internet]. Parkinsons. Dis. 2012, 1–14. [cited 2018 Jul 8] Available from. http://www.ncbi.nlm.nih.gov/pubmed/22135764.
Kim, J.I., Long, J.D., Mills, J.A., McCusker, E., Paulsen, J.S., De Soriano, I., et al., 2015. Multivariate clustering of progression profiles reveals different depression patterns in prodromal Huntington disease [Internet]. Neuropsychology 29, 949–960. [cited 2017 Mar 27] Available from. http://www.ncbi.nlm.nih.gov/pubmed/26011117.
Koolschijn, P.C.M.P., van Haren, N.E.M., Lensvelt-Mulders, G.J.L.M., Hulshoff Pol, H.E., Kahn, R.S., 2009. Brain volume abnormalities in major depressive disorder: a meta-analysis of magnetic resonance imaging studies [Internet]. Hum. Brain Mapp. 30, 3719–3735. [cited 2018 Feb 20] Available from. http://www.ncbi.nlm.nih.gov/pubmed/19441021.
la Fougère, C., Grant, S., Kostikov, A., Schirrmacher, R., Gravel, P., Schipper, H.M., et al., 2011. Where in-vivo imaging meets cytoarchitectonics: the relationship between cortical thickness and neuronal density measured with high-resolution [18F]flumazenil-PET [Internet]. Neuroimage 56, 951–960. [cited 2018 Feb 26] Available from. https://www.sciencedirect.com/science/article/pii/S105381191001445X?via%3Dihub.
Lee, H.-Y., Tae, W.S., Yoon, H.-K., Lee, B.-T., Paik, J.-W., Son, K.-R., et al., 2011. Demonstration of decreased gray matter concentration in the midbrain encompassing the dorsal raphe nucleus and the limbic subcortical regions in major depressive disorder: an optimized voxel-based morphometry study. [Internet]. J. Affect. Disord. 133, 128–136. [cited 2018 Feb 23] Available from. http://linkinghub.elsevier.com/retrieve/pii/S0165032711001583.
Leemans, A., Jones, D.K., 2009. The B-matrix must be rotated when correcting for subject motion in DTI data. Magnetic Resonance in Medicine 61 (6), 1336–1349.
Llera Arenas, A., Wolfers, T., Mulders, P., Beckmann, C.F., 2018. Inter-individual differences in human brain structure and morphometry link to population variation in demographics and behavior [Internet]. bioRxiv. https://doi.org/10.1101/413104. [cited 2018 Nov 5] Available from.
Lubeiro, A., Rueda, C., Hernández, J.A., Sanz, J., Sarramea, F., Molina, V., 2016. Identification of two clusters within schizophrenia with different structural, functional and clinical characteristics [Internet]. Prog. Neuro-Psychopharmacol. Biol. Psychiatr. 64, 79–86. [cited 2017 Mar 21] Available from. http://www.ncbi.nlm.nih.gov/pubmed/26216861.
Mahant, N., McCusker, E.A., Byth, K., Graham, S., Huntington Study Group, 2003. Huntington's disease: clinical correlates of disability and progression. [Internet]. Neurology 61, 1085–1092. [cited 2018 May 1] Available from. http://www.ncbi.nlm.nih.gov/pubmed/14581669.
Marquand, A.F., Wolfers, T., Mennes, M., Buitelaar, J., Beckmann, C.F., 2016. Beyond lumping and splitting: a review of computational approaches for stratifying psychiatric disorders [Internet]. Biol. Psychiatry Cogn. Neurosci. Neuroimaging 1, 433–447. [cited 2018 Feb 28] Available from. https://www.sciencedirect.com/science/article/pii/S2451902216300301.
Martinez-Horta, S., Perez-Perez, J., van Duijn, E., Fernandez-Bobadilla, R., Carceller, M., Pagonabarraga, J., et al., 2016. Neuropsychiatric symptoms are very common in premanifest and early stage Huntington's disease [Internet]. Park. Relat. Disord. 25, 58–64. Available from. https://doi.org/10.1016/j.parkreldis.2016.02.008.
McNally, G., Rickards, H., Horton, M., Craufurd, D., 2015. Exploring the validity of the short version of the problem Behaviours assessment (PBA-s) for Huntington's disease: a Rasch analysis [Internet]. J. Huntingtons. Dis. 4, 347–369. [cited 2018 Jul 23] Available from. http://www.ncbi.nlm.nih.gov/pubmed/26756591.
Mehrabi, N.F., Waldvogel, H.J., Tippett, L.J., Hogg, V.M., Synek, B.J., Faull, R.L.M., 2016. Symptom heterogeneity in Huntington's disease correlates with neuronal degeneration in the cerebral cortex [Internet]. Neurobiol. Dis. 96, 67–74. [cited 2017 May 9] Available from. http://linkinghub.elsevier.com/retrieve/pii/S0969996116302169.
Nana, A.L., Kim, E.H., Thu, D.C.V., Oorschot, D.E., Tippett, L.J., Hogg, V.M., et al., 2014. Widespread heterogeneous neuronal loss across the cerebral cortex in Huntington's disease. [Internet]. J. Huntingtons. Dis. 3, 45–64. [cited 2017 Mar 31] Available from. http://www.ncbi.nlm.nih.gov/pubmed/25062764.
Oliveira, A.S., Reiche, M.S., Vinescu, C.I., Thisted, S.A.H., Hedberg, C., Castro, M.N., et al., 2018. The cognitive complexity of concurrent cognitive-motor tasks reveals age-related deficits in motor performance [Internet]. Sci. Rep. 8, 6094. [cited 2018 Jul 8] Available from. http://www.nature.com/articles/s41598-018-24346-7.
Parent, A., Hazrati, L.N., 1995. Functional anatomy of the basal ganglia. I. the cortico-basal ganglia-thalamo-cortical loop. [Internet]. Brain Res. Brain Res. Rev. 20, 91–127. [cited 2019 Feb 1] Available from. http://www.ncbi.nlm.nih.gov/pubmed/7711769.
Park, J.-Y., Na, H.K., Kim, S., Kim, H., Kim, H.J., Seo, S.W., et al., 2017. Robust identification of Alzheimer's disease subtypes based on cortical atrophy patterns [Internet]. Sci. Rep. 7, 43270. [cited 2017 Mar 21] Available from. http://www.ncbi.nlm.nih.gov/pubmed/28276464.
Plummer, P., Eskes, G., Wallace, S., Giuffrida, C., Fraas, M., Campbell, G., et al., 2013. Cognitive-motor interference during functional mobility after stroke: state of the science and implications for future research. [Internet]. Arch. Phys. Med. Rehabil. 94, 2565–2574. e6. [cited 2018 Jul 8] Available from. http://www.ncbi.nlm.nih.gov/pubmed/23973751.
Ramasubbu, R., Konduru, N., Cortese, F., Bray, S., Gaxiola-Valdez, I., Goodyear, B., 2014. Reduced intrinsic connectivity of amygdala in adults with major depressive disorder. [Internet]. Front. psychiatry 5, 17. [cited 2018 Feb 23] Available from. http://www.ncbi.nlm.nih.gov/pubmed/24600410.
Scahill, R.I., Hobbs, N.Z., Say, M.J., Bechtel, N., Henley, S.M.D., Hyare, H., et al., 2013. Clinical impairment in premanifest and early Huntington's disease is associated with regionally specific atrophy [Internet]. Hum. Brain Mapp. 34, 519–529. [cited 2018

Jun 14] Available from. http://www.ncbi.nlm.nih.gov/pubmed/22102212.
Schermuly, I., Fellgiebel, A., Wagner, S., Yakushev, I., Stoeter, P., Schmitt, R., et al., 2010. Association between cingulum bundle structure and cognitive performance: an observational study in major depression [Internet]. Eur. Psychiatry 25, 355–360. [cited 2018 Feb 25] Available from. http://www.ncbi.nlm.nih.gov/pubmed/20621455.
Sockeel, P., Dujardin, K., Devos, D., Denève, C., Destée, A., Defebvre, L., 2006. The Lille apathy rating scale (LARS), a new instrument for detecting and quantifying apathy: validation in Parkinson's disease [Internet]. J. Neurol. Neurosurg. Psychiatry 77, 579–584. [cited 2018 May 19] Available from. http://www.ncbi.nlm.nih.gov/pubmed/16614016.
Smith, S.M., 2002. Fast robust automated brain extraction. Human Brain Mapping 17 (3), 143–155.
Sprengelmeyer, R., Steele, J.D., Mwangi, B., Kumar, P., Christmas, D., Milders, M., et al., 2011. The insular cortex and the neuroanatomy of major depression [Internet]. J. Affect. Disord. 133, 120–127. [cited 2018 Feb 22] Available from. http://www.ncbi.nlm.nih.gov/pubmed/21531027.
Sprengelmeyer, Orth, Müller, Wolf, Grön, Depping, et al., 2014. The neuroanatomy of subthreshold depressive symptoms in Huntington's disease: a combined diffusion tensor imaging (DTI) and voxel-based morphometry (VBM) study [Internet]. Psychol. Med. 44, 1867–1878. [cited 2018 Jun 17] Available from. http://www.ncbi.nlm.nih.gov/pubmed/24093462.
Stout, J.C., Paulsen, J.S., Queller, S., Solomon, A.C., Whitlock, K.B., Campbell, J.C., et al., 2011. Neurocognitive signs in prodromal Huntington disease. [Internet]. Neuropsychology 25, 1–14. [cited 2017 Mar 16] Available from. http://www.ncbi.nlm.nih.gov/pubmed/20919768.
Suzuki, M., Miyai, I., Ono, T., Oda, I., Konishi, I., Kochiyama, T., et al., 2004. Prefrontal and premotor cortices are involved in adapting walking and running speed on the treadmill: an optical imaging study [Internet]. Neuroimage 23, 1020–1026. [cited 2018 Jul 8] Available from. https://www-sciencedirect-com.sire.ub.edu/science/article/pii/S1053811904003672#bib23.
Taylor, W.D., MacFall, J.R., Gerig, G., Krishnan, R.R., 2007. Structural integrity of the uncinate fasciculus in geriatric depression: relationship with age of onset. [Internet]. Neuropsychiatr. Dis. Treat. 3, 669–674. [cited 2018 Feb 25] Available from. http://www.ncbi.nlm.nih.gov/pubmed/19300596.
Tippett, L.J., Waldvogel, H.J., Thomas, S.J., Hogg, V.M., W Van, Roon-Mom, Synek, B.J., et al., 2007. Striosomes and Mood Dysfunction in Huntington's Disease. pp. 206–221.
Tombaugh, T.N., 2004. Trail Making Test A and B: normative data stratified by age and education. Arch. Clin. Neuropsychol. 19, 203–214.
Torrubia, R., Ávila, C., Moltó, J., Caseras, X., 2001. The Sensitivity to Punishment and Sensitivity to Reward Questionnaire (SPSRQ) as a measure of Gray's anxiety and impulsivity dimensions. [Internet]. Pers. Individ. Dif. 31, 837–862. [cited 2018 Jul 23] Available from: https://www-sciencedirect-com.sire.ub.edu/science/article/pii/S0191886900001835.
Tu, P.-C., Chen, L.-F., Hsieh, J.-C., Bai, Y.-M., Li, C.-T., Su, T.-P., 2012. Regional cortical thinning in patients with major depressive disorder: a surface-based morphometry study. Internet Psychiatry Res. 202, 206–213. [cited 2018 Feb 20] Available from: http://linkinghub.elsevier.com/retrieve/pii/S0925492711002514.
Wagstyl, K., Ronan, L., Goodyer, I.M., Fletcher, P.C., 2015. Cortical thickness gradients in structural hierarchie. [Internet]. Neuroimage 111, 241–250. .[cited 2018 Feb 26] Available from: http://www.ncbi.nlm.nih.gov/pubmed/25725468.
Wang, R., Shen, Y., Tino, P., Welchman, A.E., Kourtzi, Z., 2017. Learning predictive statistics: strategies and brain mechanisms. [Internet]. J. Neurosci. 37, 8412–8427. [cited 2018 Jul 8] Available from: http://www.ncbi.nlm.nih.gov/pubmed/28760866.
Webb, C.A., Weber, M., Mundy, E.A., Killgore, W.D.S., 2014. Reduced gray matter volume in the anterior cingulate, orbitofrontal cortex and thalamus as a function of mild depressive symptoms: a voxel-based morphometric analysis. [Internet]. Psychol. Med. 44, 2833–2843. [cited 2018 Feb 20] Available from: http://www.journals.cambridge.org/abstract_S0033291714000348.
Winkler, A.M., Kochunov, P., Blangero, J., Almasy, L., Zilles, K., Fox, P.T., et al., 2010. Cortical thickness or grey matter volume? The importance of selecting the phenotype for imaging genetics studies. [Internet]. Neuroimage 53, 1135–1146. .[cited 2018 Feb 26] Available from: http://www.ncbi.nlm.nih.gov/pubmed/20006715.
Wolfers, T., Arenas, A.L., Onnink, A.M.H., Dammers, J., Hoogman, M., Zwiers, M.P., et al., 2017. Refinement by integration: aggregated effects of multimodal imaging markers on adult ADHD. [Internet]. J. Psychiatry Neurosci. 42, 386–394. [cited 2017 Dec 13] Available from: http://www.ncbi.nlm.nih.gov/pubmed/28832320.
Zhang, A., Leow, A., Ajilore, O., Lamar, M., Yang, S., Joseph, J., et al., 2012. Quantitative tract-specific measures of uncinate and cingulum in major depression using diffusion tensor imaging. [Internet]. Neuropsychopharmacology 37, 959–967. [cited 2018 Feb 25] Available from: http://www.ncbi.nlm.nih.gov/pubmed/22089322.